THE JOURNAL OF PHYSICAL CHEMISTRY Letters

pubs.acs.org/JPCL

Viewpoint

How to Identify, Attribute, and Quantify Triplet Defects in Ensembles of Small Nanoparticles

Cite This: *J. Phys. Chem. Lett.* 2020, 11, 7438–7442

Read Online

ACCESS | Metrics & More | Article Recommendations

ABSTRACT: Nanodiamonds containing negatively charged triplet (having an electron spin $S = 1$) nitrogen-vacancy (NV^-) centers are an extraordinary room-temperature quantum system, whose electron spins may be polarized and read out optically even in a single nanocrystal. In this Viewpoint we promote a simple but reliable method to identify, attribute, and quantify these triplet defects in a polycrystalline sample using electron paramagnetic resonance (EPR) spectroscopy. The characterization relies on a specific "forbidden" transition ("$\Delta M_S = 2$"), which appears at about half the central magnetic field and shows a remarkably small anisotropy. In particular, we emphasize that this method is by far not limited to NV^- centers in diamond but could become an important characterization tool for novel triplet defects in various types of nanoparticles.

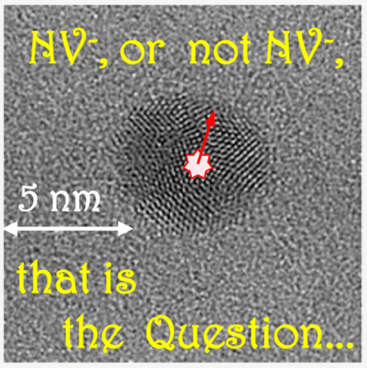

Nanodiamonds (NDs) containing negatively charged nitrogen-vacancy (NV^-) centers are a highly fascinating and unique quantum system. The NV^- center is a solid-state defect, which shows fluorescence and, in addition, allows optical polarization and readout of its electron spin states ($S = 1$) using a dedicated fluorescence microscope. The detection of a single NV^- center at room temperature lies at the basis of the state-of-the-art most sensitive magnetic resonance experiments at ambient conditions.[1,2] When such an NV^- center can be engineered in an ND particle, the whole quantum system will be incorporated into a nanoscale object. NDs containing NV^- centers are promising quantum sensors for many physical and chemical properties[3] such as temperature[4] or pH,[5] to mention only a few. The variety of new applications in the area of biology, especially as nontoxic sensors inside living cells,[6] is expected to further increase in the near future.

Recently, an observation of an optically detected magnetic resonance (ODMR) signal at room temperature from an ensemble of silicon carbide (SiC) nanoparticles as small as 3–6 nm has been reported.[7] The origin of this signal is assigned to a divacancy defect (V_C-V_{Si}) having the same triplet electron state ($S = 1$) as the NV^- center in diamond. It is exciting to see that, besides NDs, other semiconductor nanocrystals can be engineered to show an ODMR signal, notably at room temperature. We take here the opportunity to discuss the aforementioned results; compare them to the situation of NV^- centers in NDs; and, especially, comment on identification, attribution, and quantification of triplet-state ($S = 1$) defects in small nanocrystals.

Formation of NV^- centers in nitrogen-containing diamond particles is a two-step process involving creation of vacancies in the diamond lattice by electron or ion irradiation and further annealing at high temperature (usually around 800 °C) under vacuum to render vacancies mobile. While larger NDs of about 100 nm in size can be produced with hundreds of NV^- centers embedded, the small "single-digit" NDs (i.e., with a diameter smaller than 10 nm) are much more challenging to be successfully turned into a host for an NV^- center. A simple look at the given NV^- concentration in larger NDs of a few atomic ppm (in units of atomic ratio) makes it clear that not each 5-nanometer-sized ND (made of ~8000 carbon atoms) will statistically include an NV^- defect. In addition, the formation of an NV^- center in smaller NDs has a lower probability than in larger ones, because during annealing vacancies will be more often "lost" via the crystal surface because of the large surface-to-volume ratio.[8]

There are two basic methods for quantification/estimation of the content of NV centers in relatively large NDs: (i) single-particle technique and (ii) bulk or ensemble technique. In the former, individual particles are studied by a fluorescent microscope. The intensity of the characteristic fluorescence emission from an individual spot is proportional to the number of NV centers. Photoluminescence (PL) spectra provide unique assignment of fluorescent defects in NDs. The two fluorescent charge states of an NV center, NV^0 and NV^-, can be discriminated by their PL spectra. The charge state is the key identity of an "NV molecule": while NV^- is a spin triplet in its ground state ($S = 1$), NV^0 is a spin doublet ($S = 1/2$).

Received: June 20, 2020
Accepted: August 11, 2020
Published: August 11, 2020

https://dx.doi.org/10.1021/acs.jpclett.0c01922
J. Phys. Chem. Lett. 2020, 11, 7438–7442

Importantly, only the NV^- center shows an ODMR signal, which characteristically appears at the zero-field splitting of D = 2.87 GHz when no external magnetic field is applied. Such single-particle measurements are time-consuming, because numerous particles have to be scanned, until a representative average is obtained. For small NDs, an additional difficulty arises: the majority of the NDs has no NV centers and, thus, are "dark," i.e., invisible to a fluorescent microscope. Only a correlative image, a nanometer-resolved height scan with an atomic force microscopy (AFM) and a fluorescent image, recorded exactly at the same spot, can provide a ratio between "empty" and fluorescent NDs. Such pioneering studies were performed for NDs manufactured by static high-pressure high-temperature (HPHT) synthesis of micrometer-sized diamond particles followed by milling and separation,[9] as well as for NDs synthesized by a dynamic detonation technique (DNDs).[10] In both cases, individual single-digit NDs (with smallest diameters of 7.5 nm[9] and 5 nm,[10] respectively) showed a characteristic ODMR signal. However, the validity of the single-particle PL technique to estimate NV^- content in small NDs remains quite doubtful. Thus, ref 9 imparted that "35% of the nanocrystals contain a fluorescent defect center." At the same time, the AFM image in ref 9 clearly demonstrates larger ND particles presented there. Thus, according to our deep conviction, the use of the aforementioned ratio causes strong overestimation of the actual yield of NV^- centers in real "single-digit" NDs. Moreover, because all "fluorescent defects" are contributed to the count, other "bright species" like NV^0 centers might be included as well. For the DNDs 5 nm in size, the value of "0.005−0.012 ppm" as a yield in NV^- centers has been mentioned.[7,11] It is important to note that those two yield values reported cannot be compared directly. In fact, the "35%" from ref 9 is *the number of fluorescent defects per NDs* whereas "0.005−0.012 ppm" is given in the units of atomic ratio and stands for *the number of NV^- centers per Carbon atoms*. The latter number originally stems from the estimation based on optical measurements of an ND ensemble, providing "1 NV^- center per (15 ± 7) thousands nanodiamonds" which corresponds to ca. 0.007% *in NV^- centers per DNDs*.[12] To complete the confusion, we have estimated the number of NV^- centers in a pristine (not irradiated, not annealed) DND sample as ca. 1 per 1000 particles using electron paramagnetic resonance (EPR) spectroscopy.[11]

In this Viewpoint, we draw attention to the technique based on continuous-wave (CW) EPR spectroscopy to identify, attribute, and quantify NV^- centers in ensembles of small NDs. For such an ensemble of particles carrying NV^- centers with electron spin S = 1 and zero field splitting D = 2.87 GHz, one would expect a polycrystalline EPR pattern represented by the simulated spectrum in Figure 1a. However, in various DND samples a magnetic field sweep of 200 mT around g = 2 does not reveal any signal, which could be attributed to NV^-.[13] The only detectable line there, which may be related to the NV^- centers, is observed in the "half-field" region at about 159 mT (g = 4.26), slightly below half the central field at g = 2 (ca. 338 mT).[14] This line corresponds to so-called "forbidden" (or, in fact, "partially allowed") "ΔM_S = 2" transition between Zeeman sublevels. This transition occurs because of superpositions of M_S = +1 and M_S = −1 states, which result from a state mixing when the zero-field splitting D cannot be neglected compared to the microwave photon energy $h\nu$ (ν = 9−10 GHz at X-band frequency). Here it is worth mentioning that the "ΔM_S = 2" transition should not be

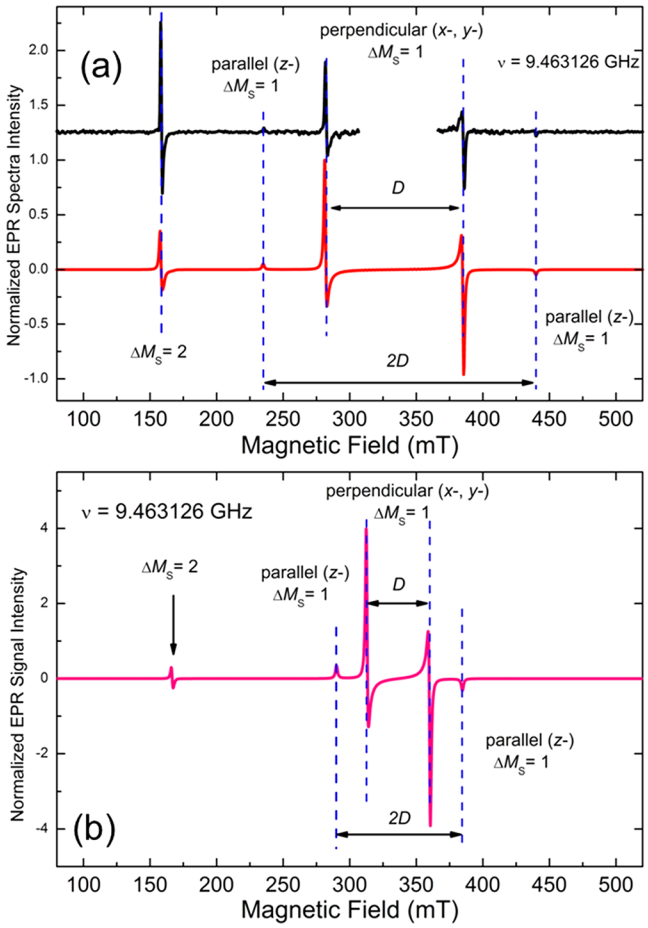

Figure 1. (a) CW EPR spectra of triplet NV^- centers in polycrystalline Ib HPHT diamond sample: black trace, experimental spectrum of the micrometer-sized electron irradiated and annealed diamond particles. Spectrum recorded at T = 295 K; microwave power, 200 μW; amplitude of 100 kHz magnetic field modulation, 1 mT; single scan, ν = 9.463126 GHz. Broad signal due to ferromagnetic impurities has been subtracted, and intense signals within g = 2.00 region are excluded; red trace, simulation of the experimental spectrum using the *pepper* function in EasySpin[16] using spin-Hamiltonian parameters typical for triplet NV^- centers: g_{iso} = 2.0028, D = 0.09585 cm^{-1} (2.87 GHz), E = 0, individual Lorentzian line width 1 mT. Inconsistency in the ratio of "allowed" and "forbidden" lines' peak intensities between the experimental and simulated spectra originates from the partial saturation of the "allowed" lines at spectra recording as well as from the presence of larger crystallites in the diamond sample. In the NV^- spectrum, the intense lines at around 280 and 380 mT are low- and high-field "allowed" ΔM_S = 1 transitions, separated by the zero-field splitting D (in mT), with the $N-V$ axis perpendicular to the external magnetic field (x-, y-lines). The weaker lines around 235 mT and 440 mT are allowed ΔM_S = 1 transitions, separated by twice the zero-field splitting 2D (in mT), with the $N-V$ axis parallel to the external magnetic field (z-lines). All these four lines are *not* visible in an experimental spectrum of 5 nm-sized DND particles. The only detectable line is the "ΔM_S = 2" "half-field" transition at about 159 mT, slightly below half the central field. (b) EasySpin simulation of CW EPR powder spectrum of a divacancy in SiC with spin-Hamiltonian parameters typical for triplet divacancies in SiC: $g_{\|}$ = 2.0041, $g_{\perp}$ = 2.0040, D = 0.04428 cm^{-1} (1.327 GHz), E = 0, individual Lorentzian line width 1 mT, ν = 9.463126 GHz. For these centers, the pattern is the same as in the panel (a), but the allowed perpendicular lines are split by ∼47 mT, which corresponds to the smaller D = 1.327 GHz value. The "half-field" transition appears at about 167 mT corresponding to g = 4.06.

https://dx.doi.org/10.1021/acs.jpclett.0c01922
J. Phys. Chem. Lett. 2020, 11, 7438−7442

confused with a "double-quantum transition", where two photons are needed for excitation: it is a conventional single-quantum transition, where only a single photon is absorbed (see Figure 2). Observation of "$\Delta M_S = 2$" transitions in a bulk

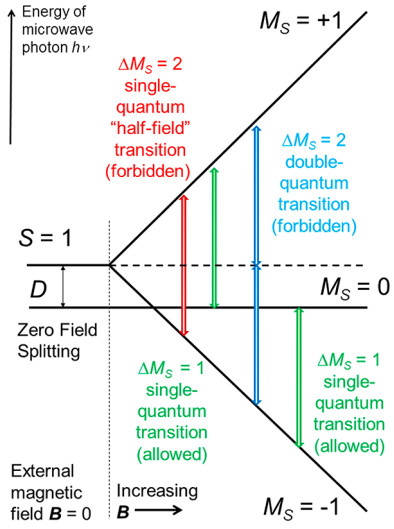

Figure 2. Different types of EPR transitions in an electron spin $S = 1$ system. Red arrow indicates $\Delta M_S = 2$ "half-field" transition appearing at half the central magnetic field or slightly lower (corresponding to $g \geq 4$). It is a "forbidden" transition between the energy levels $M_S = \pm 1$. It is a single-quantum transition; only one photon is absorbed. This becomes partially allowed when the zero-field splitting D has a comparable energy to the exciting microwave photon $h\nu$. This is the transition of interest in this Viewpoint, because its anisotropy is very small in powder samples. Green arrows indicate low- and high-field $\Delta M_S = 1$ transitions which are "allowed" transitions between the energy levels $M_S = 0$ and $M_S = \pm 1$; blue arrows indicate $\Delta M_S = 2$ double-quantum transition appearing at the g-value of the electron $g \approx 2$. It is a "forbidden" transition between the energy levels $M_S = \pm 1$, which involves absorption of two photons at a time. This transition needs a strong microwave field amplitude B_1 and is not observed in our experiments.[15]

crystalline sample requires the static magnetic field $\mathbf{B_0}$ and the microwave field $\mathbf{B_1}$ being parallel, in contrast with $\mathbf{B_0} \perp \mathbf{B_1}$, required for "allowed" $\Delta M_S = 1$ transitions. However, in a polycrystalline sample, $\mathbf{B_0}$ is randomly oriented to the principal axis and spin−spin/exchange interactions cause superposition of $M_S = +1$, $M_S = -1$, and $M_S = 0$ states which allows observation of "$\Delta M_S = 2$" transitions in the conventional EPR setup.[15] The anisotropy of the "$\Delta M_S = 2$" transition is more than an order of a magnitude smaller than for the "allowed" $\Delta M_S = 1$ transitions. This feature enables detection of "forbidden" signals in a randomly oriented sample of $S = 1$ species, even when the "allowed" transitions are invisibly broadened or masked by intense signals due to other paramagnetic species and ferromagnetic impurities. The latter "masking" is exactly the case for the NV^- centers in small NDs. The resonant magnetic field of the "$\Delta M_S = 2$" transition contains valuable information about the zero-field splittings D and E of the observed spin system.[15] The whole powder EPR spectrum can be simulated using, for example, the EasySpin software[16] (see simulated spectra in Figure 1). The lower is the microwave frequency ν; the larger is the deviation from the true "half-field" value ($g = 4$) toward lower fields (higher g values). Using this field dependence of the "$\Delta M_S = 2$" transition, the "half-field" line in DNDs was assigned to the NV^- center.[13] Thus, thorough analysis of both position and shape of "forbidden" EPR lines allows unambiguous identification of triplet centers observed in particulate nanosized samples. It may be claimed that in regard to identification of triplet centers in polycrystalline samples, careful treatment of the "forbidden" half-field lines provides the same information that could be extracted from the analysis of "allowed" lines, i.e., zero field splitting values, g-factors, and line widths. The "half-field EPR" technique allows easy discrimination between different triplet centers and estimation of their relative contributions.[17]

Speaking of nanoemitters, the second most important task (after reliable identification of a type of a triplet center) is to correctly attribute the emitters specifically to small nanoparticles. Indeed, all existing techniques for synthesis of nanosized particulates (even dynamic types of synthesis like detonation and laser ablation) result in polycrystalline ensembles, which usually contain a certain (but insignificant, as estimated by HRTEM, XRD, and DLS) content of larger particles. On discussing results of any ensemble/bulk characterization techniques (EPR, for instance) a strict consistency of the full set of experimental data must be observed. Indeed, to which particles does the effect observed really belong to? As an example, ref 7 reports on observation of two satellite lines in the EPR spectrum of the ensemble of SiC nanocrystals. These lines were attributed to SiC divacancy with a zero-field splitting $D = 1.327$ GHz. However, a true powdered sample consisting of particles with the average size of 4 nm must provide a totally angularly averaged polycrystalline EPR pattern like that in Figure 1b. Such an EPR spectrum is completely independent of the orientation of the bulk sample in the cavity. In the above case the satellite lines with splitting of the order of D definitely originate from "perpendicular" "allowed" x-, y-transitions (by convention, the external magnetic field $\mathbf{B_0}$ is set parallel to the z-direction). In a polycrystalline EPR pattern, the resonance fields of such lines are fixed and determined only by values of zero field splittings, disregarding any sample's orientation (see simulated spectra in Figure 1). Reference 7 and the Supporting Information therein report that these lines were found to be angularly dependent. Based on our experience gained from thousands of EPR measurements done on various micro- and nanodiamonds, we may conclude that the angular dependence observed in the experiments reported cannot originate from paramagnetic centers located in nanosized particles but undoubtedly indicates the attribution of those triplet centers observed to larger crystallites. The inconsistencies noted above cast doubt on the correctness of the attribution of triplet centers, responsible for ODMR in the SiC samples under study, to "ultrasmall nanocrystals," especially because we have never observed allowed transitions from NV^- centers in single-digit nanodiamonds.

After the ODMR active triplet centers have been reliably identified and attributed precisely to small nanocrystals, the question of a quantitative assessment of those triplet centers' content arises. Thus, in ref 7, a single-particle analysis for the "determination of the defects' yield in nanoparticles" was exploited. PL spectra on the drop-cast samples allowed tracking the conversion of E centers (V_C-C_{Si}) to divacancies (V_C-V_{Si}) induced by annealing at 140 °C for 2h. The conversion yield from E center to divacancy was found to be ~60%.[7] However, this number says nothing on the "total defect yield", which has been discussed for NV^- centers in

https://dx.doi.org/10.1021/acs.jpclett.0c01922
J. Phys. Chem. Lett. 2020, 11, 7438−7442

NDs. Are there also multiple "empty" SiC nanoparticles which initially did not contain any E center—an obligatory precursor of the ODMR-active divacancy? As discussed above, there are two methods that could help answering this question: a correlative AFM/fluorescence microscopy screening of individual particles, or, the measurement of the EPR "half-field" transition in a powder sample of SiC nanoparticles at different stages. The EPR method is inexpensive and requires only a CW EPR spectrometer, if possible combined with a microwave resonator having a high quality factor. As a drawback, bulk quantities of several milligrams are needed to obtain a satisfying signal-to-noise ratio within a reasonable experimental time. For DND, we usually had about 20 mg and accumulated a "half-field" EPR spectrum for a few hours. E-beam irradiated and annealed micrometer sized diamonds were found to be a proper "concentration reference" for triplet centers. EPR spectra of irradiated microdiamonds demonstrate well-resolved lines for both "allowed" and "forbidden" transitions (see, for instance, black trace in Figure 1a), which gives the opportunity to directly estimate the total amount of NV^- centers by spectral integration. It was found that the double integral of the "half-field" line is proportional to the total amount of triplet centers that is allowed using just the "half-field" line for quantification of NV^- defects in a powder sample of irradiated micro- and nanodiamonds.[18] The "half-field" line-based quantification technique seems to be as reliable as the direct double integration of the main triplet pattern as comparison shows. An independent confirmation is impossible in cases where only the "half-field" line is observable. The cumulative error in the determination of triplet spins' content does not exceed 15%.[17,18] The aforementioned technique has been also applied to study the effect of electron irradiation and annealing on 5 nm DND.[11] We were able to observe a linear increase in the concentration of NV^- center (see Figure 1 in ref 11). Two further observations are noteworthy. First, the NV^- content in the pristine (i.e., before any irradiation and/or annealing) DND is found to be significantly above zero. This confirms previous findings on an NV^- formation process which accompanies the detonation synthesis.[10,13,19,20] As mentioned above, the estimation provided that at least 1 among 1000 DND particles contains an NV^- center. Second, no significant difference in the NV^- contents with or without annealing was found. Both observations are unique to DNDs and highlight their distinction comparing to all other types of diamond. Answering the allegation in ref 7, it is worth mentioning that for DNDs elevated temperatures can be safely avoided and are *not* necessary for the creation of additional NV^- centers.[11]

It would be very interesting to study the "half-field" transition for the divacancy defect in the samples containing ultrasmall SiC nanoparticles. The position of the half-field line will confirm the identity of the divacancy as well as changes in the line intensity may be used for "tracking" the formation of useful triplet centers, as it was demonstrated for NV^- centers in micro- and nanodiamonds.[18] We are certainly expecting such a line having much better signal-to-noise ratio than the wide-field scans shown in ref 7. The obvious limitation of the "half-field" EPR method is the following: all optical effects caused by laser-excitation, such as blinking and bleaching, associated with photoionization processes, are not observed, because it is an experiment "in the dark". Therefore, even if a suitable number of NV^- centers would be detected by EPR, it is still possible that they may be hardly observed using fluorescence detection. While this might be seen as a drawback, it helps to separate two effects: (i) presence of NV^- centers in the dark and (ii) observability of NV^- centers in PL experiments. This distinction is valuable on targeted engineering of defects in ultrasmall nanocrystals. Another constraint, which one should keep in mind, is the omnipresent size distribution of the particles. Even in disaggregated DNDs known for their narrow size and shape distribution,[21] particle size measurements such as DLS reveal a tiny amount of larger particles. In a bulk measurement, one cannot know if the signal of a defect is evenly distributed over all particle sizes or if there is a bias toward larger ones. This question can be answered only by a correlative AFM/fluorescence measurement of a larger number of single isolated particles.

With the tremendous success of the NV^- center in the field of quantum science, the search for even better or complementary solid-state qubits has started. Just earlier this year, Gottscholl et al. reported for the first time an ODMR signal from an $S = 1$ defect with a zero-field splitting of $D = 3.5$ GHz in two-dimensional hexagonal boron nitride (2D hBN) at room temperature.[22] If the nanonization of such a system would succeed,[23] the "half-field" EPR method would be predestined for a fast and simple characterization of these particles. The method might not be limited to $S = 1$ defects only: EPR lines with similar low anisotropy should appear for other spins with integer values such as "$\Delta M_S = 4$" transitions in $S = 2$ electron spins.[24] Other candidates could be semiconductor nanocrystals showing an ODMR signal, structurally similar to the well-known quantum dots, which have been studied for already more than two decades.[25] Or finally, we may take the long way back to the discovery of the "half-field" transition and look at organic nanocrystals containing molecules with optically excitable electron triplet states.[26] "Forbidden" transitions between triplet state's sublevels are of great interest not only as a tool for searching and identifying triplet centers (which is the subject of this report), but also as a promising tool for spin manipulations. The remarkably low anisotropy of the "half-field" (therein called "overtone") transition could be of great use for efficient optical dynamic nuclear polarization from NV^- centers to nuclear spins in an ensemble of randomly oriented NDs.[27] Very similar to our experiments, the half-field transitions allow one to excite many NV/nanodiamond orientations, within a limited sweep width.

We are convinced that the NV^- center in nanodiamonds will retain its standing as a unique system in the quantum world. On the other hand, we are excited and curious to see that many competitive systems will be discovered in the coming years.

Takuya F. Segawa orcid.org/0000-0001-5507-3360
Alexander I. Shames orcid.org/0000-0002-0574-1911

AUTHOR INFORMATION

Complete contact information is available at:
https://pubs.acs.org/10.1021/acs.jpclett.0c01922

Notes

The authors declare no competing financial interest.

ACKNOWLEDGMENTS

T.F.S. acknowledges The Branco Weiss Fellowship—Society in Science, administered by the ETH Zurich.

REFERENCES

(1) Gruber, A.; Dräbenstedt, A.; Tietz, C.; Fleury, L.; Wrachtrup, J.; von Borczyskowski, C. Scanning Confocal Optical Microscopy and

Magnetic Resonance on Single Defect Centers. *Science* **1997**, *276*, 2012−2014.
(2) Jelezko, F.; Gaebel, T.; Popa, I.; Gruber, A.; Wrachtrup, J. Observation of Coherent Oscillations in a Single Electron Spin. *Phys. Rev. Lett.* **2004**, *92*, 076401.
(3) Schirhagl, R.; Chang, K.; Loretz, M.; Degen, C. L. Nitrogen-Vacancy Centers in Diamond: Nanoscale Sensors for Physics and Biology. *Annu. Rev. Phys. Chem.* **2014**, *65*, 83−105.
(4) Kucsko, G.; Maurer, P. C.; Yao, N. Y.; Kubo, M.; Noh, H. J.; Lo, P. K.; Park, H.; Lukin, M. D. Nanometre-Scale Thermometry in a Living Cell. *Nature* **2013**, *500*, 54−58.
(5) Rendler, T.; Neburkova, J.; Zemek, O.; Kotek, J.; Zappe, A.; Chu, Z.; Cigler, P.; Wrachtrup, J. Optical Imaging of Localized Chemical Events Using Programmable Diamond Quantum Nanosensors. *Nat. Commun.* **2017**, *8*, 14701.
(6) Fu, C.-C.; Lee, H.-Y.; Chen, K.; Lim, T.-S.; Wu, H.-Y.; Lin, P.-K.; Wei, P.-K.; Tsao, P.-H.; Chang, H.-C.; Fann, W. Characterization and Application of Single Fluorescent Nanodiamonds as Cellular Biomarkers. *Proc. Natl. Acad. Sci. U. S. A.* **2007**, *104*, 727−732.
(7) Beke, D.; Valenta, J.; Károlyházy, G.; Lenk, S.; Czigány, Z.; Márkus, B. G.; Kamarás, K.; Simon, F.; Gali, A. Room-Temperature Defect Qubits in Ultrasmall Nanocrystals. *J. Phys. Chem. Lett.* **2020**, *11*, 1675−1681.
(8) Smith, B. R.; Inglis, D. W.; Sandnes, B.; Rabeau, J. R.; Zvyagin, A. V.; Gruber, D.; Noble, C. J.; Vogel, R.; Ōsawa, E.; Plakhotnik, T. Five-Nanometer Diamond with Luminescent Nitrogen-Vacancy Defect Centers. *Small* **2009**, *5*, 1649−1653.
(9) Tisler, J.; Balasubramanian, G.; Naydenov, B.; Kolesov, R.; Grotz, B.; Reuter, R.; Boudou, J. P.; Curmi, P. A.; Sennour, M.; Thorel, A.; et al. Fluorescence and Spin Properties of Defects in Single Digit Nanodiamonds. *ACS Nano* **2009**, *3*, 1959−1965.
(10) Bradac, C.; Gaebel, T.; Naidoo, N.; Sellars, M. J.; Twamley, J.; Brown, L. J.; Barnard, A. S.; Plakhotnik, T.; Zvyagin, A. V.; Rabeau, J. R. Observation and Control of Blinking Nitrogen-Vacancy Centres in Discrete Nanodiamonds. *Nat. Nanotechnol.* **2010**, *5*, 345−349.
(11) Terada, D.; Segawa, T. F.; Shames, A. I.; Onoda, S.; Ohshima, T.; Ōsawa, E.; Igarashi, R.; Shirakawa, M. Monodisperse Five-Nanometer-Sized Detonation Nanodiamonds Enriched in Nitrogen-Vacancy Centers. *ACS Nano* **2019**, *13*, 6461−6468.
(12) Smith, B. R.; Gruber, D.; Plakhotnik, T. The Effects of Surface Oxidation on Luminescence of Nano Diamonds. *Diamond Relat. Mater.* **2010**, *19*, 314−318.
(13) Shames, A. I.; Osipov, V. Yu.; von Bardeleben, H.-J.; Boudou, J.-P.; Treussart, F.; Vul', A. Ya. Native and Induced Triplet Nitrogen-Vacancy Centers in Nano- and Micro-Diamonds: Half-Field Electron Paramagnetic Resonance Fingerprint. *Appl. Phys. Lett.* **2014**, *104*, 063107.
(14) Osipov, V. Yu.; Shames, A. I.; Enoki, T.; Takai, K.; Baidakova, M. V.; Vul', A. Ya. Paramagnetic Defects and Exchange Coupled Spins in Pristine Ultrananocrystalline Diamonds. *Diamond Relat. Mater.* **2007**, *16*, 2035−2038.
(15) Weil, J. A.; Bolton, J. R. *Electron Paramagnetic Resonance*, 2nd ed.; John Wiley & Sons, Inc., 2007.
(16) Stoll, S.; Schweiger, A. EasySpin, a Comprehensive Software Package for Spectral Simulation and Analysis in EPR. *J. Magn. Reson.* **2006**, *178*, 42−55.
(17) Shames, A. I.; Smirnov, A. I.; Milikisiyants, S.; Danilov, E. O.; Nunn, N.; McGuire, G.; Torelli, M. D.; Shenderova, O. Fluence-Dependent Evolution of Paramagnetic Triplet Centers in e-Beam Irradiated Microcrystalline Ib Type HPHT Diamond. *J. Phys. Chem. C* **2017**, *121*, 22335−22346.
(18) Shames, A. I.; Osipov, V. Yu.; Boudou, J. P.; Panich, A. M.; von Bardeleben, H. J.; Treussart, F.; Vul', A. Ya. Magnetic Resonance Tracking of Fluorescent Nanodiamond Fabrication. *J. Phys. D: Appl. Phys.* **2015**, *48*, 155302.
(19) Shames, A. I.; Osipov, V. Yu.; von Bardeleben, H. J.; Vul', A. Ya. Spin S = 1 Centers: A Universal Type of Paramagnetic Defects in Nanodiamonds of Dynamic Synthesis. *J. Phys.: Condens. Matter* **2012**, *24*, 225302.
(20) Reineck, P.; Capelli, M.; Lau, D. W. M.; Jeske, J.; Field, M. R.; Ohshima, T.; Greentree, A. D.; Gibson, B. C. Bright and Photostable Nitrogen-Vacancy Fluorescence from Unprocessed Detonation Nanodiamond. *Nanoscale* **2017**, *9*, 497−502.
(21) Krüger, A.; Kataoka, F.; Ozawa, M.; Fujino, T.; Suzuki, Y.; Aleksenskii, A. E.; Vul', A. Ya.; Ōsawa, E. Unusually Tight Aggregation in Detonation Nanodiamond: Identification and Disintegration. *Carbon* **2005**, *43*, 1722−1730.
(22) Gottscholl, A.; Kianinia, M.; Soltamov, V.; Orlinskii, S.; Mamin, G.; Bradac, C.; Kasper, C.; Krambrock, K.; Sperlich, A.; Toth, M.; et al. Initialization and Read-out of Intrinsic Spin Defects in a van der Waals Crystal at Room Temperature. *Nat. Mater.* **2020**, *19*, 540−545.
(23) Joni, I. M.; Balgis, R.; Ogi, T.; Iwaki, T.; Okuyama, K. Surface Functionalization for Dispersing and Stabilizing Hexagonal Boron Nitride Nanoparticle by Bead Milling. *Colloids Surf., A* **2011**, *388*, 49−58.
(24) Hagen, W. R. EPR of Non-Kramers Doublets in Biological Systems: Characterization of an S = 2 System in Oxidized Cytochrome c Oxidase. *Biochim. Biophys. Acta, Protein Struct. Mol. Enzymol.* **1982**, *708*, 82−98.
(25) Lifshitz, E.; Fradkin, L.; Glozman, A.; Langof, L. Optically Detected Magnetic Resonance Studies of Colloidal Semiconductor Nanocrystals. *Annu. Rev. Phys. Chem.* **2004**, *55*, 509−557.
(26) Nishimura, K.; Kouno, H.; Tateishi, K.; Uesaka, T.; Ideta, K.; Kimizuka, N.; Yanai, N. Triplet Dynamic Nuclear Polarization of Nanocrystals Dispersed in Water at Room Temperature. *Phys. Chem. Chem. Phys.* **2019**, *21*, 16408−16412.
(27) Jeong, K.; Parker, A. J.; Page, R. H.; Pines, A.; Vassiliou, C. C.; King, J. P. Understanding the Magnetic Resonance Spectrum of Nitrogen Vacancy Centers in an Ensemble of Randomly Oriented Nanodiamonds. *J. Phys. Chem. C* **2017**, *121*, 21057−21061.

https://dx.doi.org/10.1021/acs.jpclett.0c01922
J. Phys. Chem. Lett. 2020, 11, 7438−7442